Analytica Chimica Acta 1068 (2019) 87–95

Contents lists available at ScienceDirect

Analytica Chimica Acta

journal homepage: www.elsevier.com/locate/aca

A novel fluorescence aptasensor based on mesoporous silica nanoparticles for selective and sensitive detection of aflatoxin B_1

Hongxia Tan, Liang Ma*, Ting Guo, Hongyuan Zhou, Lu Chen, Yuhao Zhang, Hongjie Dai, Yong Yu

College of Food Science, Southwest University, Chongqing, 400715, China

HIGHLIGHTS

- High amino-modified concentration of mesoporous silica nanomaterials (MSN-NH_2) was synthesized.
- MSN-NH_2 loaded with label-free signal probe (Rh6G) could be regulated by gated molecular (AFB_1-aptamers).
- This aptasensor is designed by MSN-NH_2, Rh6G and AFB1-aptamers to detect AFB1 with the detection limit of 0.13 ng mL^{-1}.
- This design could be applied to other mycotoxins and contaminants if appropriate aptamers are available.

GRAPHICAL ABSTRACT

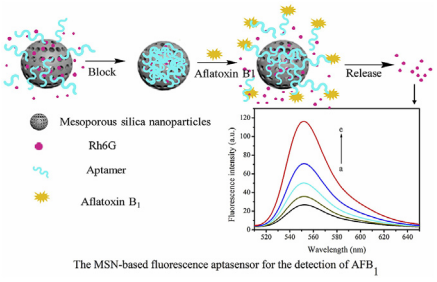

The MSN-based fluorescence aptasensor for the detection of AFB_1

ARTICLE INFO

Article history:
Received 3 January 2019
Received in revised form
13 March 2019
Accepted 8 April 2019
Available online 11 April 2019

Keywords:
Aptasensor
Aflatoxin B_1
Modified mesoporous silica nanoparticles
Gated control
Label-free

ABSTRACT

Based on the mesoporous silica nanoparticles (MSN), a novel, simple and label-free aptamer biosensor was designed for the detection of aflatoxin B_1 (AFB_1). Here, the aptamers were used as molecular recognition probes and "gated molecules" while Rh6G was loaded into the interior of the particles as the signal probe. In the absence of AFB_1, the "gate" was closed to prevent the leakage of the signal probe because of the immobilization of aptamers on the surface of MSN-NH_2. With the presence of AFB_1, the "gate" could be opened to release the signal probe for the specifical binding of aptamers to AFB_1. Our results showed that the fluorescence intensity was positively correlated with the concentration of AFB_1 (0.5–50 ng mL^{-1}), with the detection limit as low as 0.13 ng mL^{-1}. What's more, this design provides a new approach for rapid, sensitive and selective detection based on aptamers and it could be applied to numerous other analytes if appropriate aptamers are available.

1. Introduction

Mycotoxins, as the toxic and carcinogenic secondary metabolites produced by various molds, can cause serious problems to human health by contaminating numerous foods and animal feeds [1,2]. In recent years, aflatoxins often have been found in agricultural products, raising many global concerns due to a series of economic losses and potential risk to foods and feeds [3]. Among several types of aflatoxins, AFB_1, as the most toxic carcinogen, has been classified as Group I carcinogen by International Agency for Research on Cancer (IARC) [4]. Generally, agricultural products, such as, peanuts, corn and grains are particularly vulnerable to AFB_1

* Corresponding author. No.2 Tiansheng Road, Beibei District of ChongQing, 400715, China.
E-mail addresses: zhyhml@swu.edu.cn, zhyhml@163.com (L. Ma).

https://doi.org/10.1016/j.aca.2019.04.014
0003-2670/

contamination [5]. The maximum contamination levels of AFB_1 (2 μg kg^{-1}) and total aflatoxins (4 μg kg^{-1}) in all cereal and cereal-based products have been determined by European Commission to safeguard consumers' health and avoid food safety risk [6]. Up to date, the main methods for the detection of AFB_1 are typically instrumental approaches, such as, high performance liquid chromatography (HPLC) [7–9], liquid chromatography combined with mass spectrometry (LC-MS) [10], as well as rapid detection technologies, like enzyme-linked immunosorbent assays (ELISA) [11,12] and so on. These methods can accurately detect the presence of AFB_1, however, tedious pretreatments, expensive equipment and professional operator are required [13,14]. Besides, antibody-based rapid analyses require expensive, laborious and time-consuming antibody preparation and also may be susceptible to the instability of the antibody. In this case, the design of a simple, rapid, sensitive and cost-effective method for quantifying AFB_1 has become a research hotspot.

Aptamer, a single-stranded DNA or RNA oligonucleotide sequence, has high affinity and specificity for targets [15]. Owing to their higher affinity, lower cost, easier modification and higher stability [16], aptamers are being explored as a highly promising alternative to antibody [17]. Besides, aptamers can be functionalized with all kinds of fluorophores [18], functional groups [19], biotin and enzymes [20], which could simplify the inspection procedures and make the sensing platform more flexible. Thus, aptamers have been adopted as novel molecular recognition probes for the detection of mycotoxins. Up to now, aptamer-based biosensors have been developed for the detection of several mycotoxins, such as AFB_1 [21–23], AFM_1 [24,25], ochratoxin A (OTA) [26], zearalenone (ZEN) [27,28] and so on.

Significantly, giving the credit to the ease of modification, good biocompatibility and uniform nanometer size of nanoparticles (magnetic nanoparticles, silica nanoparticles, grapheme, and etc.), many sensor strategies based on nanoparticles have been established to detect various mycotoxins [29]. Mesoporous silica nanomaterials (MSN) have been widely used for their large surface area, good thermal stability, easy modification, good porosity, large load capacity, and excellent reactivity [30,31]. Chen et al. [32] took advantage of the porosity of the MSN as a carrier molecule in conjunction with chemiluminescence to determine cocaine. And also, S. Dehghani et al. [33] established the MSN-based sensor to detect kanamycin.

Based on these ideas, we report herein for the first time that an aptasensor based on MSN has been developed for detection of AFB_1 in this paper. MSN was firstly synthesized and then the MSN-based controlled release system was combined with the specific aptamers of AFB_1 to construct an aptasensor. Here, the aptamers are used as molecular recognition probes and "gated molecules". The affinity of the specific binding of aptamers-AFB_1 is greater than the electrostatic force of aptamers and MSN, which could make the "gate" open to release the Rh6G. The quantitative detection of AFB_1 is achieved by the enhancement of fluorescence intensity. The whole sensing procedures are simple, rapid and highly specific to AFB_1, which offers a great potential for on-site analysis.

2. Experimental

2.1. Materials and apparatus

Aflatoxin B_1 (AFB_1), Aflatoxin B_2 (AFB_2) were purchased from Sigama (USA). Aflatoxin M_1 (AFM_1), Deoxynivalenol (DON), Zearalenone (ZEN), Ochratoxin (OTA), Fumotoxin B_1 (FB_1), T-2 were purchased from Pribolab (Singamore). Other chemical reagents such as cetyltrimethylammonium (CTAB), tetraethyloxysilane (TEOS), 3-amino-propyltriethoxysilane (APTES), Rhodamine 6G (Rh6G) were obtained from Aladdin Reagent Co. Ltd., (Shanghai, China). Disodium phosphate (Na_2HPO_4), Sodium dihydrogen phosphate (NaH_2PO_4) and Sodium hydroxide (NaOH) were obtained from Cologne Chemical Co. Ltd (Chengdu, China). The samples of peanut oil, corn oil, corn, peanut, oatmeal, rice were purchased from the local supermarket (Chongqing, China). The AFB_1 aptamers (Apt1, Apt2, Apt3, Apt4, Apt5) used in this work (Table 1) were synthesized and purified with HPLC by Shanghai Sangon Biotechnology Co. Ltd. (Shanghai, China). All other chemicals were at analytical grade and aqueous solutions were prepared with ultrapure water (18.25 MΩ*cm).

The transmission electron microscopy (TEM) images were obtained with JEM-1200EX (Japan). FTIR spectra of the nanoparticles were obtained with Spectrum 100 (PerkinElmer, USA). Ultraviolet–visible (Uv–vis) absorption spectra were collected by UV-2450 (Shimadzu, Japan). The zeta potential was recorded on ZEN3690 (Malvern, England). Fluorescent intensity measurements were performed by F02500 (Shimadzu, Japan). Accuracy of this method was verified by HPLC on LC-20A (Shimadzu, Japan).

2.2. Synthesis of MSN

In this study, MSN was synthesized with the reported procedures with slight modifications [39–46]. Briefly, MSN was synthesized under alkaline conditions using TEOS as a silica precursor, CTAB as a surfactant template, NaOH as a catalyst and water as a solvent. Firstly, 0.5 g of CTAB was initially dissolved in 240 mL ultrapure water with slowly stirring at 80 °C to get a clear and transparent solution. Afterwards, 1.75 mL of NaOH (2 M) and 2.5 mL of TEOS were added dropwisely to the mixture solution, followed by vigorously stirring for 2 h. The mixture was allowed to stand for cooling, and then centrifuged at 10000 rpm for 10 min. The resulting product was washed successively with ethanol and water three times to remove the remaining solvent from the pores. MSN containing the template CTAB was obtained by vacuum drying overnight. The above prepared MSN nanoparticles were calcined at 550 °Cfor 5.5 h to remove the excess surfactant CTAB.

2.3. Synthesis of amino-modified MSN (MSN-NH_2)

0.5 g of MSN was homogeneously dispersed in 50 mL of ethanol by ultrasonication. After that, 1.5 mL of APTES was added into the mixture solution with slowly stirring for 10 h at 110 °C. Then, the white solid was recovered via centrifugation at 8000 rpm for 10 min, followed by washing with ethanol and water three times to

Table 1
Aptamer used in this study.

NO	Sequence (5′-3′)	Reference
Apt 1	AGTTGGGCACGTGTTGTCTCTCTGTGTCTCGTGCCCTTCGCTAGGCCCACA	[34]
Apt 2	GTT GGG CAC GTG TTG TCT CTC TGT GTC TCG TGC CCT TCG CTA GGC CC	[35]
Apt 3	CAG AGA GAC AAC ACG TGC CCA AC	[36]
Apt 4	ATA GGA GTC ACG ACG ACC AGA AAG TAA TGC CCG GTA GTT ATT CAA AGA TGA GTA GGA AAG ATA TGT GCG TCT ACC TCT TGA CTA	[37]
Apt 5	TTG GGC ACG TGT TGT CTC TCT GTG TCT CGT GCC CTT CGC TAG GCC CAC A	[38]

remove the excess APTES. Finally, MSN-NH_2 was obtained in a vacuum freeze-drying oven. The concentration of amino-modified on the MSN was calculated [32].

2.4. Preparation of the fluorescent aptasensor for AFB_1 detection

To fabricate the MSN-based aptasensor, 30 mg of MSN-NH_2 was incubated with 500 μL of Rh6G solution (1 mM) with shaking for 14 h at 25 °C. After that, the MSN-NH_2/Rh6G complex was incubated with 200 μL of a 100 μM aptamer capture probe for 5 h at 25 °C. The complexes of aptamer/MSN-NH_2/Rh6G were formed, centrifuged and washed repeatedly with ultrapure water to remove excess aptamers and Rh6G dye. Finally, the above complexes were resuspended in phosphate saline (PBS, 0.2 M, pH 7.4) ($C_{[MSN\text{-}NH2]} = 60\ mg\ mL^{-1}$) for further using.

The process of AFB_1 detection was carried out as follows. Firstly, 50 μL of the above particle dispersion solution was added into 600 μL of AFB_1 solution diluted in PBS. 600 μL of PBS was added as a blank control. After fully shaking, the mixture solution was then incubated at 37 °C for 3 h. The corresponding fluorescent intensity at excitation/emission wavelength of 490/552 nm was recorded at room temperature (25 °C).

2.5. Sample analysis

In order to evaluate the recovery of the MSN-based fluorescence aptasensor, the samples of peanut oil, corn oil, corn, peanut, oatmeal and rice were obtained from supermarket. First of all, the samples were detected by HPLC to verify the presence of AFB_1. Afterwards, each of corn oil and corn samples was spiked with AFB_1 at the concentration of 1, 3, 5, ng mL^{-1}, respectively. Each spiked sample (5.00 ± 0.005 g) and 25 mL of the extraction solution (methanol:water = 7:3) were mixed to extract AFB_1. The corn, peanut, oatmeal and rice were vortexed for 20 min and then extracted using ultrasonic for 30 min. Subsequently, the solution was collected. The peanut oil, corn oil were vortexed for 20 min and then extracted using ultrasonic for 30 min Then, the filtered solution was further extracted with 10 mL of n-hexane and 10 mL of 70% methanol in a separatory funnel. Finally, all extracts were collected, dried with nitrogen and diluted in PBS for AFB_1 detection.

In order to evaluate analytical reliability and applicability of the proposed MSN-based fluorescence aptasensor, the detection of AFB_1 in natural samples were carried out in accordance with the procedures above.

3. Results and discussion

3.1. The strategy of the proposed fluorescence aptasensor for AFB_1 detection

Schematic illustration for the design of MSN-based fluorescent aptasensor for AFB_1 detection was shown in Fig. 1A. MSN-NH_2 was selected as the carrier for the controlled release system and Rh6G was loaded into the interior of the particles as signal probe. As "gated molecule" and molecular recognition probes, the aptamers were immobilized on the surface of MSN-NH_2 particles based on the interaction of positively charged MSN-NH_2 with negatively charged aptamers. The aptasensor (aptamers-modified MSN-NH_2 loaded with Rh6G) was prepared for the detection of the target AFB_1. In the presence of AFB_1, the aptamers could be removed from MSN-NH_2 by the specific binding between aptamers and AFB_1, thus the "gate" was opened and signal probe (Rh6G) is released. In the case, the fluorescence intensity was positively correlated with the concentration of AFB_1 and the quantitative detection of AFB_1 could be finally achieved by the change of fluorescence intensity.

To confirmed the feasibility of the aptasensor, series concentration of AFB_1 were respectively added into the aptamer/MSN-NH_2/Rh6G complexes to obtain their corresponding fluorescent intensities. As shown in Fig. 1B, the fluorescence intensity was enhanced with the increasing concentration of AFB_1. Therefore, this principle could be applied to develop a sensitive MSN-based fluorescence aptasensor for the AFB_1 detection.

3.2. Characterization of the synthesized MSN-NH_2

The formation of mesopores mainly refers to the process of removing surfactants by high temperature treatment or other physicochemical methods [47]. As could be seen from Fig. 2A, strong absorbing peaks at 2921 cm^{-1}, 2851 cm^{-1} (C–H stretching vibration) and 1478 cm^{-1}(C–H deformation) were shown in line a, which could be caused by a large amount of surfactants residue in the porous pores. Besides, in line b, these peaks were found to be disappeared, suggesting that the mesopores were formed after the removal of surfactants [48]. Compared with MSN, MSN-NH_2 (line c) showed new peaks at 1636 cm^{-1} and 1554 cm^{-1}, corresponding to the flexural stretching vibrations of amide I and $-NH_2$, respectively. After modification of the MSN with amino groups, vibrational peaks were displayed at 1340 cm^{-1} and 1410 cm^{-1}, which could be attributed to the stretching band of the C–N group [32]. Furthermore, the Si–OH band at 962 cm^{-1} in the MSN-NH_2 spectrum became weaker after amino modification. These results suggested

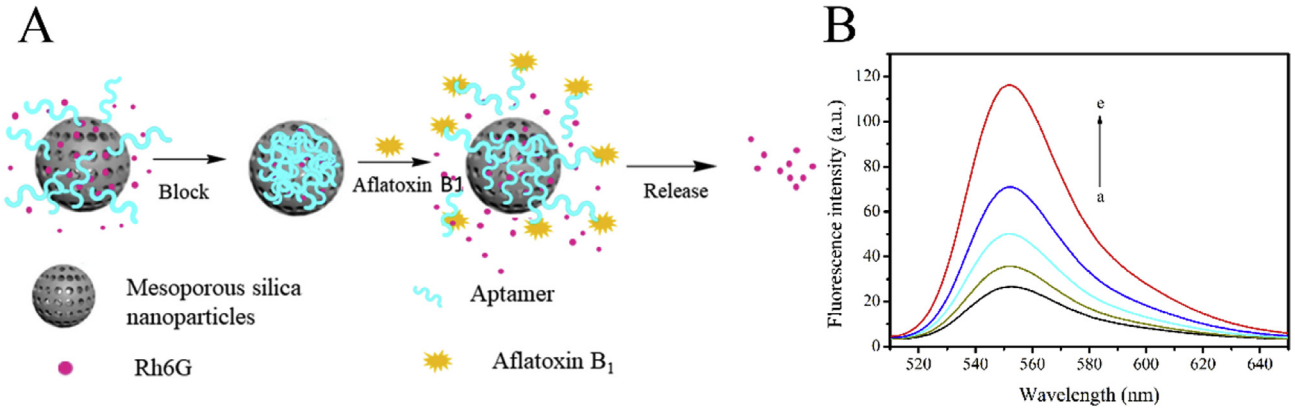

Fig. 1. (A) Principles of the MSN-based fluorescence aptasensor for the detection of AFB_1. (B) Fluorescence emission sepctra of the MSN-based fluorescence aptasensor in the presence of AFB_1 (a:0, b:5 ng mL^{-1}, c:10 ng mL^{-1}, d:20 ng mL^{-1}, e:40 ng mL^{-1}). Excitation and emission are at λex/λem = 490/552 nm.

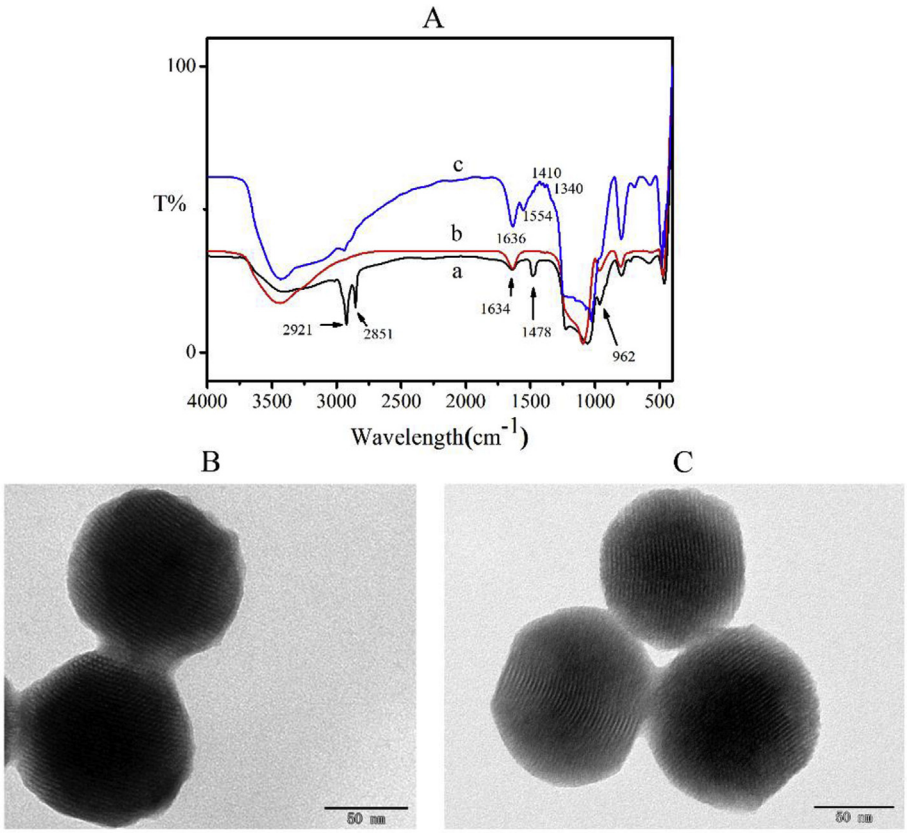

Fig. 2. (A) FTIR spectra of MSN with surfactant, MSN and MSN-NH_2 (from a to c). (B) TEM micrograph of MSN. (C) TEM micrograph of MSN-NH_2.

that amino groups were successfully modified onto MSN.

Moreover, the pores structures of MSN and MSN-NH_2 were furthered proved by TEM. Fig. 2B and C showed typical images of the synthesized MSN and MSN-NH_2, the average size of the as-synthesized nanoparticles was 100 nm. The TEM image showed that the MSN and MSN-NH_2 possessed excellent mesoporous channel structures. A large number of pores on the MSN-NH_2 indicated that the MSN-NH_2 nanoparticles had the potential applicability as a carrier to contain more fluorochrome.

The concentration of amino-modified on the MSN was 1.235 mmol g^{-1}, which was 10 times of other MSN-NH_2 nanoparticles in the reported [32]. The modification of amino groups to MSN and the binding of aptamers to MSN-NH_2 nanoparticles were verified by zeta potential and UV spectra. As shown in Fig. 3A, the zeta potential of MSN was increased from −32 mV to 20.8 mV after modification of the MSN with amino groups. The change of the zeta potential decreased from 20.8 mV to −34.3 mV after the binding of MSN-NH_2 with aptamers, which confirmed the conjugation between aptamers and MSN-NH_2.

Moreover, the UV–vis spectra showed that aptamers were successfully bound to the MSN-NH_2. As shown in Fig. 3B, the disappearance of the characteristic absorption peak at 260 nm could be attributed to the formation of aptamer/MSN-NH_2 complex. Besides, characteristic absorption peak at 260 nm was found in the aptamer + MSN-NH_2 spectrum (Fig. 3C), illustrating the successful binding of aptamers on MSN-NH_2 nanoparticles.

3.3. Screening out AFB_1-specific aptamer suitable for MSN-based aptasensor strategy

As a recognition molecular, specificity and affinity of aptamers are the bases of the proposed aptasensor. A large number of aptamers have been selected for AFB_1 recognition by SELEX methods. Therefore, a total of five AFB_1 aptamers (Apt1, Apt2, Apt3, Apt4, Apt5) were selected to investigate its specificity and affinity in the proposed method. They are commonly used and reported in the previous literature. The specificity of this aptasensor for AFB_1 and its analogues, aflatoxin B_2 (AFB_2), OTA, ZEN and deoxynivalenol (DON) was evaluated using the proposed aptasensor strategy at the same test conditions (Fig. 4A). As shown in Fig. 4A, the specificity of aptamers in the proposed biosensor was evaluated with 30 ng mL^{-1} of the mycotoxins. AFB_1 induced the highest fluorescence intensity with binding to Apt1 (the black column in Fig. 4A) while the other analogues (AFB_2, DON, ZEN or OTA) induced a low fluorescence intensity. This indicated that Apt1 can strongly bound to AFB_1 but only slightly bind with other mycotoxins. In particular, AFB_2 contains almost the same carbon skeleton as AFB_1, except for the double bond on the difuradin ring. However, the fluorescence intensity of AFB_1 was still up to fourteen-fold higher than that of AFB_2 when Apt1 (black column in Fig. 4A) was used as the recognition sequence. The other four aptamers tested (Apt2, Apt3, Apt4, Apt5) were also able to recognize AFB_1 (the other color columns except black), but showing much poorer specificity than Apt1. So Apt1 is the best one of the five aptamers to recognize AFB_1.

AFB_1 aptamers with different sequences (Apt1, Apt2, Apt3, Apt4, Apt5) were also investigated in affinity of aptamer recognition probe to target with proposed aptasensor. As shown in Fig. 4B, with the increasing of AFB_1 concentration, the fluorescence intensity of the tested group increased gradually. In particular, the fluorescence intensity of Apt1 and Apt2 increased more in the linear range of 0.5~50 ng mL^{-1}. It indicated that Apt1 and Apt2 had a strong affinity for AFB_1 in this aptasensor. Based on the specificity and

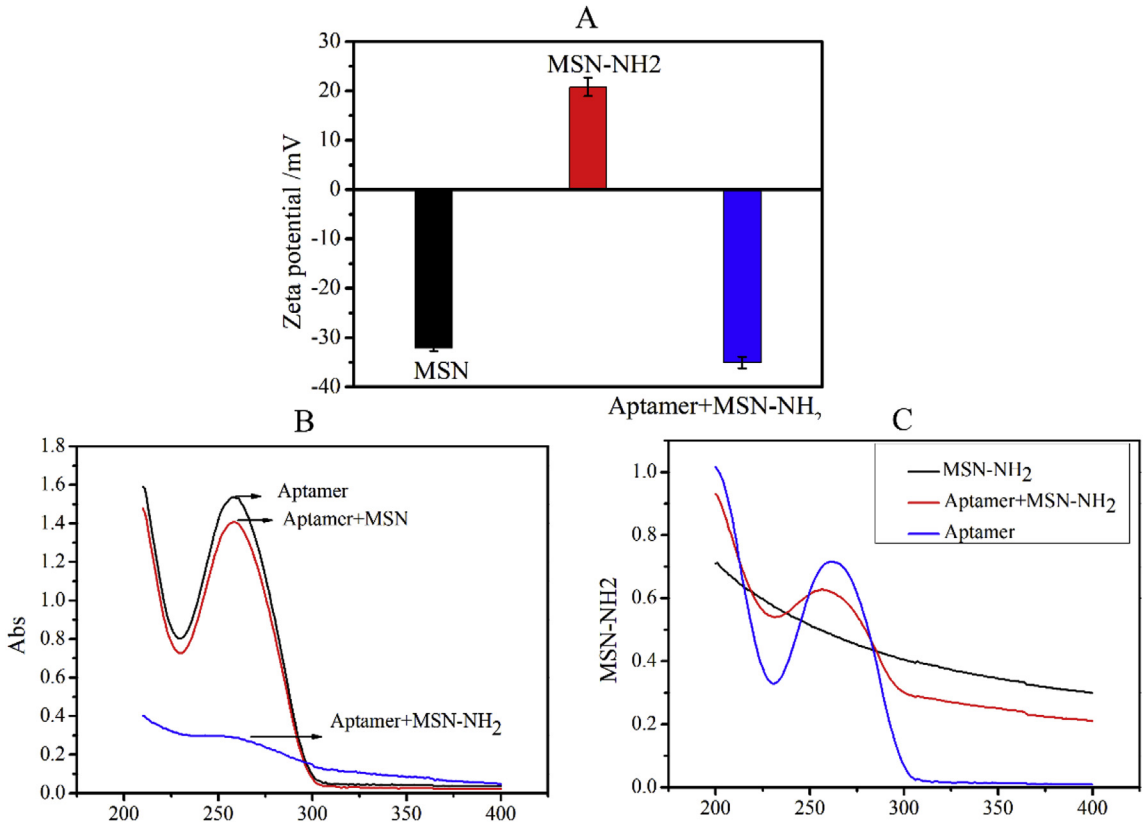

Fig. 3. (A) Zeta potential of MSN, MSN-NH_2, aptamer/MSN-NH_2 complex. (B) UV–Vis spectra of supernatant of pure aptamer, aptamer/MSN and aptamer/MSN-NH_2 complexes. (C) UV–Vis spectra of aptamer, MSN-NH2 and aptamer/MSN-NH_2.

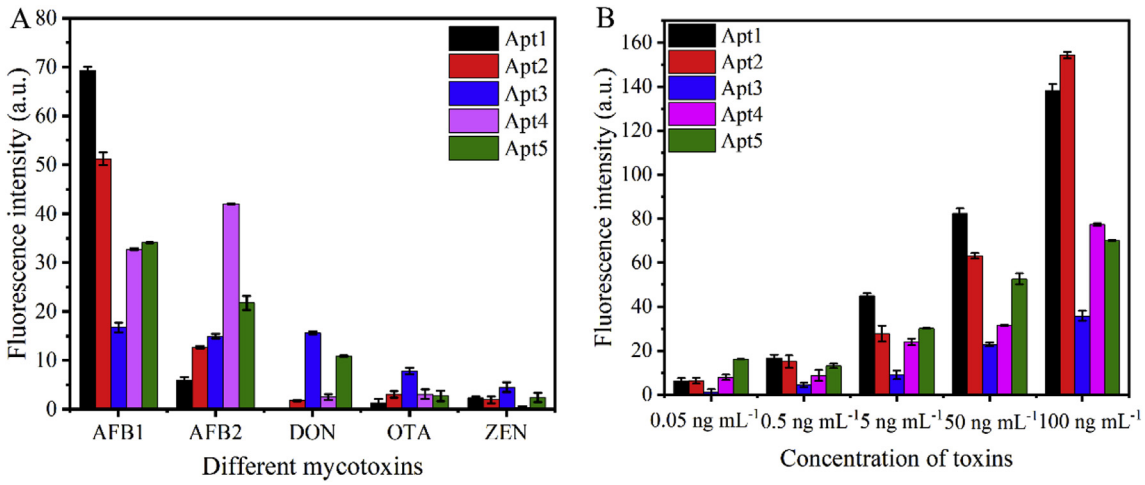

Fig. 4. (A) Evaluation of selectivity of the proposed MSN-based aptasensor for AFB_1 (each of mycotoxins was 30 ng mL^{-1}). (B) Evaluation of affinity of the proposed MSN-based aptasensor for AFB_1.

affinity of aptamers for the proposed method, Apt1 was selected as the molecular recognition probe of this designed aptasensor for the following experiments.

3.4. Study of experimental parameters

In order to improve the performance of the aptasensor, we investigated the recovery efficiency of the fluorescence intensity after the combination of different concentrations of Apt1 and MSN-NH_2. As shown in Fig. 5A, with the increase of Apt1 concentration from 0 μM to 120 μM, the recovery value of the fluorescence intensity in the sensor system was gradually enhanced. The recovery value of the fluorescence intensity would be reached a plateau at a concentration over 100 μM. The reason lied in that all MSN-NH_2 nanoparticles had electrostatically combined with Apt1 when the concentration of Apt1 was 100 μM. Therefore, 100 μM was selected as the Apt1 concentration for the following experiments.

The effect of the binding time of Apt1-MSN-NH_2 on fluorescence intensity was further investigated. As shown in Fig. 5B, the fluorescence intensity was gradually enhanced and reached a

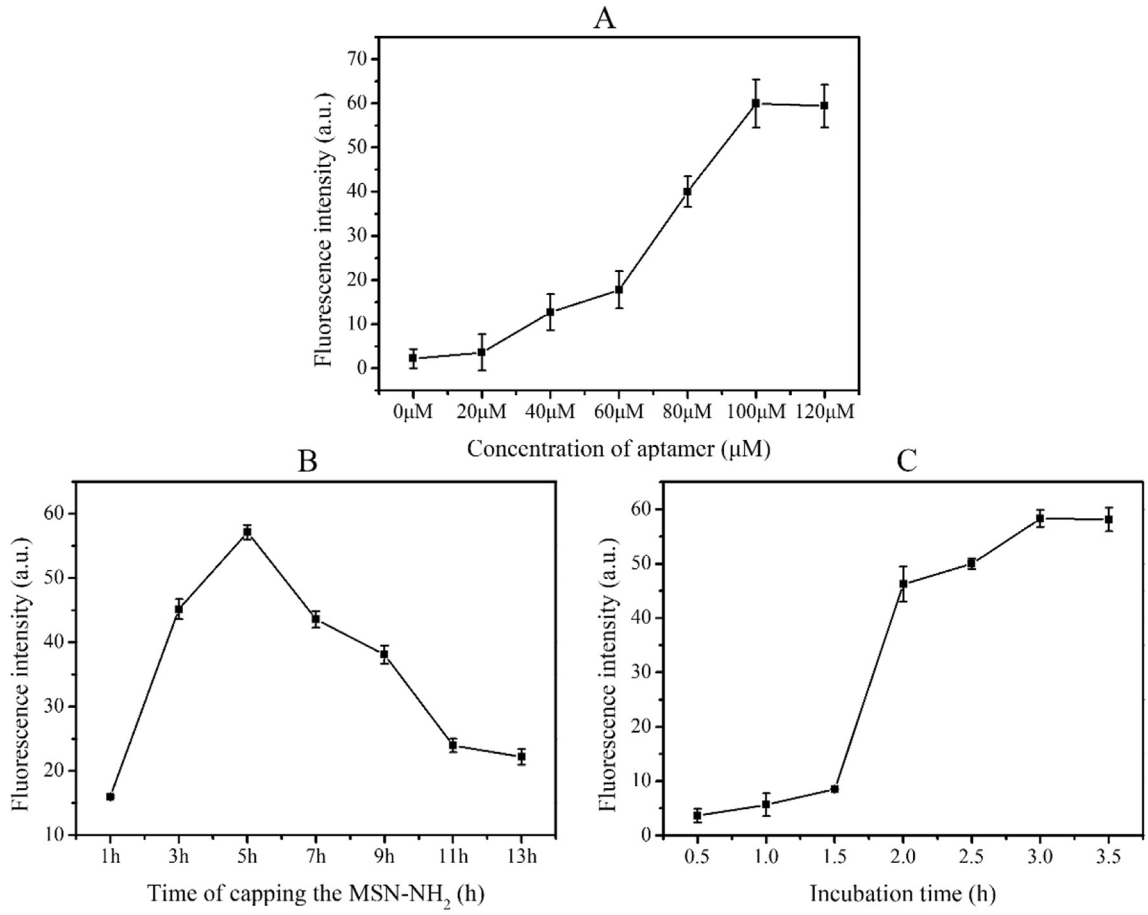

Fig. 5. (A) The effect of Apt1 concentration on the fluorescence intensity. (B) The effect of the capping time for the Apt1-MSN-NH_2 on the fluorescence intensity. (C) The effect of incubation time on the fluorescence intensity. The concentration of AFB_1 was 10 ng mL^{-1}.

maximum at 5 h. Then, the fluorescence intensity was decreased after 5 h. The phenomenon could be that the increasing Apt1 attached to the surface of MSN-NH_2 within 5 h, which improved the performance of the aptasensor. After 5 h, the interaction force between Apt1 and MSN-NH_2 was so strong that the release of signal probe Rh6G was affected. Therefore, the capping time of 5 h was selected as the Apt1 capping time for its beneficial to the sensitivity of the aptasensor.

The effect of incubation time for Apt1-AFB_1 in aptasensor on fluorescence intensity was investigated and shown in Fig. 5C. The fluorescence intensity was enhanced significantly with the incubation time consuming of AFB_1. The aptasensor had its best function based on the incubation time of 3 h for AFB_1.

3.5. Detection of AFB_1 based on MSN-NH_2 aptasensor

As shown in Fig. 6A, the fluorescence intensity of supernatant solution increased with the increasing of AFB_1. The fluorescence intensity reached a plateau when the AFB_1 concentration was up to 160 ng mL^{-1}. Besides, Fig. 6B showed a good linear correlation between the fluorescence intensity and the concentration of AFB_1 in the dynamic range of 0.5 50 ng mL^{-1}. The limit of detection (LOD) was calculated by 3 σ_b/slope (σ_b, standard deviation of the blank samples) to be 0.13 ng mL^{-1}.

The characteristics of the proposed MSN-based aptasensor were compared with other methods reported previously and summarized in Table 2. The LOD of the proposed method was barely comparable to or even lower than most of the reported methods previously. Moreover, the proposed MSN-based aptasensor was also compared with other mentods based on fluorescence [49–51] and electrochemistry [52–54]. Results showed that the analytical method in this study had wider linear range, higher sensitivity, easier sample preparation, simpler operation and less time-consuming, holding great potentials in AFB_1 rapid detection.

3.6. Specificity of the aptasensor

In order to evaluate the selectivity and specificity of this aptasensor, 20 ng mL^{-1} of mycotoxins (AFB_1, AFB_2, AFM_1, DON, OTA, ZEN, T-2) were tested under the optimized experimental conditions. As shown in Fig. 7, under the same conditions, strong fluorescence intensity of the aptasensor was only induced by AFB_1 while weak intensity was detected in the groups of both control and other mycotoxins. It was supposed that other mycotoxins could not specifically bind to AFB_1 aptamers and couldn't disrupt the electrostatic binding between MSN-NH_2 and aptamers. Thus, almost no fluorescent dye could be released into the solution to generate significantly fluorescent enhancement. Based on the results above, the MSN-based aptasensor method could eliminate the interference resulted from other mycotoxins and had a good specificity for AFB_1 determination.

3.7. Accuracy of aptasensor in samples detection

In order to evaluate the accuracy in samples detection, the proposed aptasensor was applied to determine AFB_1 in spiked corn

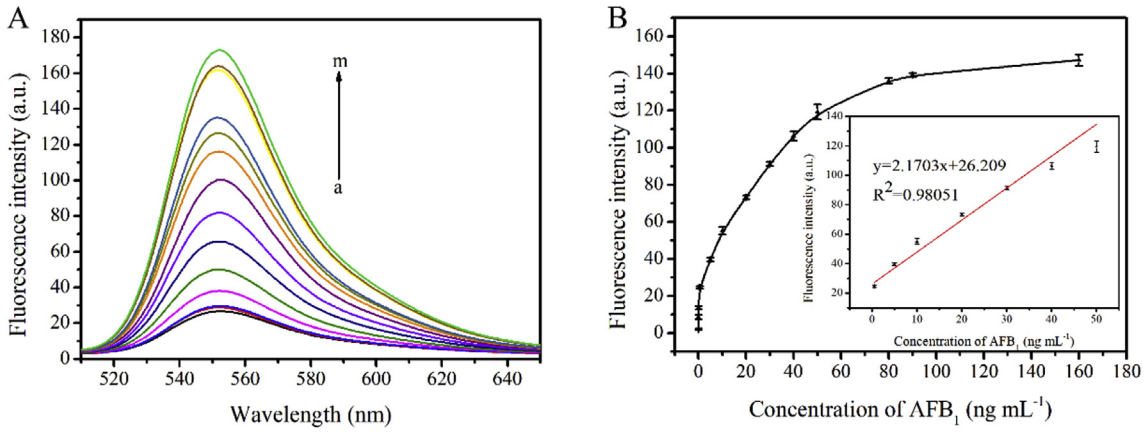

Fig. 6. (A) Fluorescence spectra of the proposed aptasensor with different concentrations (from a to m) of AFB_1: 0, 0.0005, 0.005, 0.05, 0.5, 5, 10, 20, 30, 40, 50, 80, 90, 160 ng mL^{-1}; (B) Linear relationship between the fluorescence intensity and AFB_1 concentration. Inset: a calibration curve for determination of AFB_1. Every data point was the mean of three measurements.

Table 2
Comparison of the method proposed in this study with other methods previously for AFB_1.

Methods		LOD (ng mL^{-1})	Reference
Antibody based methods	Immunochromatography assay	2.5	[55]
	Clean-up tandem immunoassay column	5	[56]
	Enzyme immunoassay	2	[57]
Aptamer based methods	A simple aptamer-based fluorescent assay	1.6	[50]
	A Rapid Label-Free Fluorescent Aptasensor	0.1	[51]
	An aptamer-based dipstick assay	0.1	[34]
	electrochemical aptasensor assay	0.25	[52]
	Aptasensor assy	0.13	This work

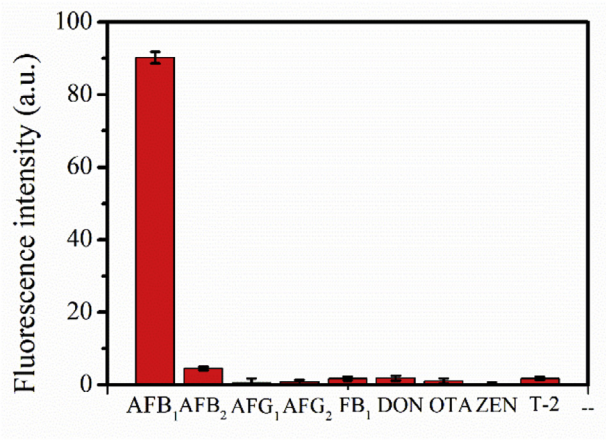

Fig. 7. Histogram of selectivity in the presence of 20 ng mL^{-1} mycotoxins: AFB_1, AFB_2, AFG_1, AFM_1, DON, OTA, ZEN, T-2. Each data point was the mean of three measurements with error bars.

oil and corn samples obtained from the local supermarket. Before the assay, the two samples were detected by HPLC to verify the absence of AFB_1. As shown in Table 3, the average recoveries of the spiked samples varied from 89.70%–94.70%.

Seven samples obtained from local supermarket were also applied to detect the concentration of AFB_1 by the aptasensor and HPLC [58] respectively (Table 4). No significant difference was found in the two methods ($P > 0.05$).

4. Conclusion

In summary, we develop a naw aptasensor for AFB_1 detection which includes aptamers as a specific recognition element, mesoporous silica nanoparticles as a carrier and Rh6G as a fluorescent indicator. Under the optimal experimental conditions, the fluorescence intensity could be linearly increased when the concentrations of AFB_1 ranging from 0.5 50 ng mL^{-1} (LOD = 0.13 ng mL^{-1}). This method will be promoted on the sensitivity and specificity for higher affinity and specificity aptamers sequence of AFB_1 obtained successfully in the future. Overall, this method could be applied for non-professional operators in a very simple mode. Besides, it

Table 3
Recoveries of AFB_1 in corn oil and corn samples for applicability of aptasensor (n = 3).

Recoveries sample	Found in sample (ng g^{-1})	Added AFB_1 (ng g^{-1})	Found AFB_1 (ng g^{-1})	% Recovery	% RSD
Corn oil	0	1	0.9	90.30	13.93
	0	3	2.84	94.70	7.02
	0	5	4.62	92.40	7.26
Corn	0	1	0.93	93.00	8.24
	0	3	2.69	89.70	7.75
	0	5	4.69	93.80	5.25

Table 4
AFB_1 contamination levels in samples.

Samples	AFB_1 contaminated levels (ng g^{-1})	
	Aptasensor	HPLC-FLD
Peanut coil	17.02	16.68
Pepper	0.09	0.08
Corn oil	ND	ND
Corn	ND	ND
Oatmeal	ND	ND
Rice	ND	ND
Peanut	ND	ND

Note:$P > 0.05$.

apparently is a low-cost method compared with the general quantitative detection method such as HPLC with immunoaffinity column. With the advantages of novel "gate" design, simple pretreatment, low cost, short time-consuming, high sensitivity and strong specificity, the developed aptasensor can be considered as a promising detection tool of AFB_1 in grain and oil products safety field.

Declaration of interests

The authors declare that they have no known competing financial interests or personal relationships that could have appeared to influence the work reported in this paper.

Funding

This work was supported by the Fundamental Research Funds for the Central Universities (Project NO. XDJK2019B028, SWU 117005 and SWU 118088).

Acknowledgements

The authors are grateful for the College of Food Science, Southwest University for the exceptional quality of the assistance provided.

References

[1] A.T. Mata, J.P. Ferreira, B.R. Oliveira, M.C. Batoreu, M.T.B. Crespo, V.J. Pereira, M.R. Bronze, Bottled water: analysis of mycotoxins by LC-MS/MS, Food Chem. 176 (2015) 455–464.
[2] R.Y. Zhu, K. Feussner, T. Wu, F.J. Yan, P. Karlovsky, X.D. Zheng, Detoxification of mycotoxin patulin by the yeast Rhodosporidium paludigenum, Food Chem. 179 (2015) 1–5.
[3] X. Zhang, C.R. Li, W.C. Wang, J. Xue, Y.L. Huang, X.X. Yang, B. Tan, X.P. Zhou, C. Shao, S.J. Ding, A novel electrochemical immunosensor for highly sensitive detection of aflatoxin B1 in corn using single-walled carbon nanotubes/chitosan, Food Chem. 192 (2016) 197–202.
[4] P.Q. Zhao, L.F. Li, S.Y. Zhao, L.H. Qiu, Z.Z. Qian, X.M. Liu, X.C. Chao, H.L. Zhang, TPGS functionalized mesoporous silica nanoparticles for anticancer drug delivery to overcome multidrug resistance, Mater. Sci. Eng. C 84 (2018) 108–117.
[5] R. Chen, F. Ma, P.W. Li, X.X. Ding, Q. Zhang, M. Li, Y.R. Wang, B.C. Xu, Effect of ozone on aflatoxins detoxification and nutritional quality of peanuts, Food Chem. 146 (2014) 284–288.
[6] O. Ketney, A. Santini, S. Oancea, Recent aflatoxin survey data in milk and milk products: a review, International Journal of Dairy Technology 70 (2017) 320–331.
[7] J.C. Vidal, L. Bonel, A. Ezquerra, S. Hernandez, J.R. Bertolin, C. Cubel, J.R. Castillo, Electrochemical affinity biosensors for detection of mycotoxins: a review, Biosens. Bioelectron. 49 (2013) 146–158.
[8] C. Ruchika, S. Jay, S. Tushar, T. Basu, B.D. Malhotra, Recent advances in mycotoxins detection, Biosens. Bioelectron. 81 (2016) 532–545.
[9] A. Laura, G. Cristina, B. Claudio, Mycotoxin detection, Curr. Opin. Biotechnol. 37 (2016) 120–126.
[10] J.N. Selvaraj, L. Zhou, Y. Wang, Y.J. Zhao, F.G. Xing, X.F. Dai, Y. Liu, Mycotoxin detection-Recent trends at global level, Journal of Integrative Agriculture 14 (2015) 2265–2281.
[11] L.J. Xie, M. Chen, Y.B. Ying, Development of methods for determination of aflatoxins, Crit. Rev. Food Sci. Nutr. 56 (2015) 2642–2664.
[12] J.N. Selvaraj, Y. Wang, L. Zhou, Y.J. Zhao, F.G. Xing, X.F. Dai, Y. Liu, Recent mycotoxin survey data and advanced mycotoxin detection techniques reported from China: a review, Food Addit. Contam. 32 (2015) 440–452.
[13] C.N. Rossi, C.R. Takabayashi, M.A. Ono, G.H. Saito, E.N. Itano, O. Kawamura, E.Y. Hirooka, E.Y. Sataque Ono, Immunoassay based on monoclonal antibody for aflatoxin detection in poultry feed, Food Chem. 132 (2012) 2211–2216.
[14] S.M. Taghdisi, N.M. Danesh, M. Ramezani, K. Abnous, A new amplified fluorescent aptasensor based on hairpin structure of G-quadruplex oligonucleotide-Aptamer chimera and silica nanoparticles for sensitive detection of aflatoxin B1, in the grape juice, Food Chem. 268 (2018) 342–346.
[15] J. Qian, C.C. Ren, C.Q. Wang, W. Chen, X.T. Liu, H. Li, Q. Liu, N. Hao, H.M. Li, K. Wang, Magnetically controlled fluorescence aptasensor for simultaneous determination of ochratoxin A and aflatoxin B1, Anal. Chim. Acta 1019 (2018) 119–127.
[16] C.Q. Wang, J. Qian, K.Q. An, C.C. Ren, X.T. Liu, N. Hao, Q. Liu, H.N. Li, X.Y. Huang, K. Wang, Fabrication of magnetically assembled aptasensing device for label-free determination of aflatoxin B1 based on EIS, Biosens. Bioelectron. 108 (2018) 69–75.
[17] M.X. Yang, G.K. Liu, H.M. Mehedi, Q.O.Y. Qin, Q.S. Chen, A universal SERS aptasensor based on DTNB labeled GNTs/Ag core-shell nanotriangle and CS-Fe3O4 magnetic-bead trace detection of Aflatoxin B1, Anal. Chim. Acta 986 (2017) 122–130.
[18] M.M. Zhao, P.L. Wang, Y.J. Guo, L.X. Wang, F. Luo, B. Qin, L.H. Guo, X.O. Su, Z.Y. Lin, G.N. Chen, Detection of aflatoxin B 1, in food samples based on target-responsive aptamer-cross-linked hydrogel using a handheld pH meter as readout, Talanta 176 (2017) 34–39.
[19] K. Abnous, N.M. Danesh, M. Alibolandi, M. Ramezani, A.S. Emrani, R. Zolfaghari, S.M. Taghdisi, A new amplified π-shape electrochemical aptasensor for ultrasensitive detection of aflatoxin B1, Biosens. Bioelectron. 94 (2017) 374–379.
[20] A. Sharma, G. Catanante, A. Hayat, G. Istamboulie, I. Ben Rejeb, S. Bhand, J.L. Marty, Development of structure switching aptamer assay for detection of aflatoxin M1 in milk sample, Talanta 158 (2016) 35–41.
[21] G. Istamboulie, N. Paniel, L. Zara, L. Reguillo Granados, L. Barthelmebs, T. Noguer, Development of an impedimetric aptasensor for the determination of aflatoxin M1 in milk, Talanta 146 (2015) 464–469.
[22] L.L. Sun, L.Q. Wu, Q. Zhao, Aptamer based surface plasmon resonance sensor for aflatoxin B1, Microchimica Acta 184 (2017) 1–6.
[23] Y.V.V.A. Kumar, R.M. Renuka, J. Achuth, V. Mudili, S. Poda, Development of a FRET-based fluorescence aptasensor for the detection of aflatoxin B1 in contaminated food grain samples, RSC Adv. 8 (2018) 10465–10473.
[24] Marco Mascini, Aptamer in Bioanalysis, Chemical Industry Press, Beijing, 2010, pp. 1–278. M.
[25] L. Ma, T. Guo, S.L. Pan, Y.H. Zhang, A fluorometric aptasensor for patulin based on the use of magnetized graphene oxide and DNase I-assisted target recycling amplification, Microchimica Acta 235 (2018) 79–85.
[26] J. Zhang, Y.K. Xia, M. Chen, D.Z. Wu, S.X. Cai, M.M. Liu, W.H. He, J.H. Chen, A fluorescent aptasensor based on DNA-scaffolded silver nanoclusters coupling with Zn(II)-ion signal-enhancement for simultaneous detection of OTA and AFB1, Sensor. Actuator. B Chem. 235 (2016) 79–85.
[27] F.S. Sabet, M. Hosseini, H. Khabbaz, M. Dadmehr, M.R. Ganjali, FRET-based aptamer biosensor for selective and sensitive detection of aflatoxin B1 in peanut and rice, Food Chem. 220 (2017) 527–532.
[28] A. Ribes, S. Santiago-Felipe, A. Bernardos, M.D. Msrcos, T. Pardo, F. Sancenon, R. Martinez-Manez, E. Aznar, Two new fluorogenic aptasensors based on capped mesoporous silica nanoparticles to detect ochratoxin A, Chemistryopen 6 (2017) 653–659.
[29] A. Ribes, E. Aznar, A. Bernardos, M.D. Marcos, P. Amoros, R. Martinez-Manez, F. Sancenon, Fluorogenic sensing of carcinogenic bisphenol A using aptamer-capped mesoporous silica nanoparticles, Chem. Eur J. 23 (2017) 8581–8584.
[30] R.R. Castillo, A. Baeza, M. Vallet-Regi, Recent applications of the combination of mesoporous silica nanoparticles with nucleic acids: development of bio-responsive devices, carriers and sensors, Biomaterials Science 5 (2017) 353–377.
[31] N. Poonia, V. Lather, D. Pandita, Mesoporous silica nanoparticles: a smart nanosystem for management of breast cancer, Drug Discov. Today 23 (2017) 315–332.
[32] Z.H. Chen, Y. Tan, K.F. Xu, L. Zhang, B. Qiu, L.H. Guo, Z.Y. Lin, G.N. Chen, Stimulus-response mesoporous silica nanoparticle-based chemiluminescence biosensor for cocaine determination, Biosens. Bioelectron. 75 (2016) 8–14.
[33] S. Dehghani, N.M. Danesh, M. Ramezani, M. Alibolandi, P. Lavaee, M. Nejabat, K. Abnous, S.M. Taghdisi, A label-free fluorescent aptasensor for detection of kanamycin based on dsDNA-capped mesoporous silica nanoparticles and Rhodamine B, Anal. Chim. Acta 1030 (2018) 142–147.
[34] Q. Li, Z.C. Liu, X.C. Tan, X.Y. Xiao, P. Wang, L. Wu, K. Shao, W.M. Yin, H.Y. Han, Ultrasensitive detection of aflatoxin B1 by SERS aptasensor based on exonuclease-assisted recycling amplification, Biosens. Bioelectron. 97 (2017) 59–64.
[35] Q.S. Chen, M.X. Yang, X.J. Yang, H.H. Li, Z.M. Guo, M.H. Rahma, A large Raman scattering cross-section molecular embedded SERS aptasensor for ultrasensitive Aflatoxin B1 detection using CS-Fe3O4 for signal enrichment, Spectrochim. Acta Mol. Biomol. Spectrosc. 189 (2017) 147–153.
[36] Y.V.V.A. Kumar, R.M. Renuka, J. Achuth, M. Venkataramana, M. Ushakiranmayi,

P. Sudhakar, Development of hybrid IgG-aptamer sandwich immunoassay platform for aflatoxin B1 detection and its evaluation onto various field samples, Front. Pharmacol. 9 (2018) 1–11.
[37] M. Mukherjee, P. Bhatt, H.K. Manonmani, Fluorescent competitive aptasensor for detection of aflatoxin B1, J. Mol. Recognit. 30 (2017) 1–6.
[38] N.V. Beloglazova, E.S. Speranskaya, A. Wu, Z. Wang, M. Sanders, V.V. Goftman, D. Zhang, I.Y. Goryacheva, S. De Saeger, Novel multiplex fluorescent immunoassays based on quantum dot nanolabels for mycotoxins determination, Biosens. Bioelectron. 62 (2014) 59–65.
[39] M.A. Moreno-Villaecija, J. Sedo-Vegara, E. Guisasola, A. Baeza, M. Vallet Regi, F. Nador, D. Ruiz-Molina, Polydopamine-like coatings as payload gatekeepers for mesoporous silica nanoparticles, ACS Appl. Mater. Interfaces 10 (2017) 7761–7769.
[40] W.Q. Li, L.P. Sun, Y.Q. Xia, S.J. Hao, G. Cheng, Z.G. Wang, Y. Wan, Z.D. Zhu, H.Z. He, S.Y. Zheng, Pre-occupation of empty carriers decreases endo/lysosome escape and reduces the protein delivery efficiency of mesoporous silica nanoparticles, ACS Appl. Mater. Interfaces 10 (2018) 5430–5437.
[41] Z.H. Chen, M. Sun, F. Luo, K.F. Xu, Z.Y. Lin, L. Zhng, Stimulus-response click chemistry based aptamer-functionalized mesoporous silica nanoparticles for fluorescence detection of thrombin, Talanta 178 (2017) 563–568.
[42] P.Y. Zhao, L.D. Cao, D.K. Ma, Z.L. Zhou, Q.L. Huang, C.P. Pan, Translocation, distribution and degradation of prochloraz-loaded mesoporous silica nanoparticles in cucumber plants, Nanoscale 10 (2017) 1798–1806.
[43] I.M.M. Kenawy, Y.G. Abou El-Reash, M.M. Hassanien, N.R. Alnagar, W.I. Mortada, Use of microwave irradiation for modification of mesoporous silica nanoparticles by thioglycolic acid for removal of cadmium and mercury, Microporous Mesoporous Mater. 258 (2017) 217–227.
[44] S. Karimi, M. Heydari, Voltammetric mixture analysis of tyrosine and tryptophan using carbon paste electrode modified by newly synthesized mesoporous silica nanoparticles and clustering of variable-partial least square: efficient strategy for template extraction in mesoporous silica nanoparticle synthesis, Sensor. Actuator. B Chem. 257 (2018) 1134–1142.
[45] W. Alejandro Talavera-Pech, A. Esparza-Ruiz, P. Quintana-Owen, A. Rafael Vilchis-Nestor, C. Carrera-Figueiras, A. Avila-Ortega, Effects of different amounts of APTES on physicochemical and structural properties of amino-functionalized MCM-41-MSNs, J. Sol. Gel Sci. Technol. 80 (2016) 1–12.
[46] F. Albertini, T. Ribeiro, C. Baleizao, J.P.S. Farinha, Boron-chelating membranes based in hybrid mesoporous silica nanoparticles for water purification, Mater. Des. 141 (2018) 407–413.
[47] Z. Gounani, M.A. Asadollahi, R.L. Meyer, A. Arpanaei, Loading of polymyxin B onto anionic mesoporous silica nanoparticles retains antibacterial activity and enhances biocompatibility, Int. J. Pharm. 537 (2017) 148–161.
[48] C. Chen, W. Sun, X.L. Wang, Y.B. Wang, P. Wang, Rational design of curcumin loaded multifunctional mesoporous silica nanoparticles to enhance the cytotoxicity for targeted and controlled drug release, Mater. Sci. Eng. C 85 (2018) 88–96.
[49] L. Chen, F. Wen, M. Li, X.D. Guo, S.L. Li, N. Zheng, J.Q. Wang, A simple aptamer-based fluorescent assay for the detection of Aflatoxin B1 in infant rice cereal, Food Chem. 215 (2017) 377–382.
[50] C. Zhang, X.W. Dou, M.F. Sun, M. Zhao, O.Y. Zhen, D.D. Kong, F.L. Antonio, M.H. Hua, A rapid label-free fluorescent aptasensor PicoGreen-based strategy for aflatoxin B_1 detection in traditional Chinese medicines, Toxins 10 (2018) 101–113.
[51] W.B. Shim, M.J. Kim, H. Mun, M.G. Kim, An aptamer-based dipstick assay for the rapid and simple detection of aflatoxin B1, Biosens. Bioelectron. 62 (2014) 288–294.
[52] K.Y. Goud, G. Catanante, A. Hayat, M. Satyanarayana, K.V. Gobi, J.L. Marty, Disposable and portable electrochemical aptasensor for label free detection of aflatoxin B1 in alcoholic beverages, Sensor. Actuator. B Chem. 235 (2016) 466–473.
[53] Z.M. Li, Z.Z. Ye, Y.C. Fu, Y.H. Xiong, Y.B. Li, A portable electrochemical immunosensor for rapid detection of trace aflatoxin B1 in rice, Analytical Methods 8 (2015) 548–553.
[54] G. Castillo, K. Spinella, A. Poturnayova, M. Snejdarkova, L. Mosiello, T. Hianik, Detection of aflatoxin B1 by aptamer-based biosensor using PAMAM dendrimers as immobilization platform, Food Control 52 (2015) 9–18.
[55] L.A. Corcuera, M. Ibanez-Vea, A. Vettorazzi, E. Gonzalez-Penas, A. Lopez de Cerain, Validation of a UHPLC-FLD analytical method for the simultaneous quantification of aflatoxin B1 and ochratoxin a in rat plasma, liver and kidney, J. Chromatogr. B 879 (2011) 2733–2740.
[56] X.L. Sun, X.L. Zhao, J. Zhou, F.S. Chu, Preparation of gold-labeled antibody probe and its use in immunochromatography assay for detection of aflatoxin B1, Int. J. Food Microbiol. 99 (2005) 185–194.
[57] I.Y. Goryacheva, S. De Saeger, B. Delmulle, M. Lobeau, S.A. Eremin, I. Barna-Vetro, C. Van Peteghem, Simultaneous non-instrumental detection of aflatoxin B1 and ochratoxin A using a clean-up tandem immunoassay column, Anal. Chim. Acta 590 (2007) 118–124.
[58] D. Saha, D. Acharya, D. Roy, D. Shrestha, T.K. Dhar, Simultaneous enzyme immunoassay for the screening of aflatoxin b1 and ochratoxin a in chili samples, Anal. Chim. Acta 584 (2007) 343–349.